Microbial species interactions determine community diversity in fluctuating environments

Shota Shibasaki[1], Mauro Mobilia[2], and Sara Mitri[1]

[1]Department of Fundamental Microbiology, University of Lausanne, Switzerland

[2]Department of Applied Mathematics, School of Mathematics, University of Leeds, United Kingdom

E-mail addresses of all authors.

SS: shota.shibasaki@unil.ch

MM: M.Mobilia@leeds.ac.uk

SM: sara.mitri@unil.ch

Short running title: Microbial diversity under fluctuation

Key words: competitive exclusion, environmental switching, demographic noise, chemostat, beta diversity, intermediate disturbance hypothesis

Type of article: article

Numbers of words: 150 words in abstract, and 5052 words in main text.

Number of references: 53.

Numbers of figures: 4, tables: 1, text box 0.

Corresponding author: Sara Mitri: Quartier UNIL-Sorge, Batiment Biophore, Office 2414, CH-1015 Lausanne. Phone : +41 21 692 56 12. E-mail: sara.mitri@unil.ch.

Statement of authorship: SS, MM and SM designed the study, SS performed simulations, analyzed data, and wrote the first draft, and all authors contributed to revisions.

Abstract

Microorganisms often live in environments that fluctuate between mild and harsh conditions. Although such fluctuations are bound to cause local extinctions and affect species diversity, it is unknown how diversity changes at different fluctuation rates and how this relates to changes in species interactions. Here, we use a mathematical model describing the dynamics of resources, toxins, and microbial species in a chemostat where resource supplies switch. Over most of the explored parameter space, species competed, but the strength of competition peaked at either low, high, or intermediate switching rates depending on the species' sensitivity to toxins. Importantly, however, the strength of competition in species pairs was a good predictor for how community diversity changed over the switching rate. In sum, predicting the effect of environmental switching on competition and community diversity is difficult, as species' properties matter. This may explain contradicting results of earlier studies on the intermediate disturbance hypothesis.

1 Introduction

Natural environments are not static: temperature, pH, or availability of resources change over time. Many studies in microbiology, ecology and evolution have focused on responses to fluctuations in resource abundance in the regime of feast and famine periods (Hengge-Aronis, 1993; Vasi et al., 1994; Srinivasan and Kjelleberg, 1998; Xavier et al., 2005; Merritt and Kuehn, 2018; Himeoka and Mitarai, 2019). These models capture the dynamics within many natural ecosystems. For example, the gut microbiome of a host is exposed to fluctuating resources that depend on its host's feeding rhythm, which may affect microbiota diversity (Cignarella et al., 2018; Li et al., 2017; Thaiss et al., 2014). In addition to their magnitude, environmental fluctuations can also differ in their time scales: for the gut microbiota, a host's feeding rhythm may vary from hourly to daily, or even monthly if feeding depends on seasonal changes (Davenport et al., 2014; Smits et al., 2017). Finally, the host does not always feed its gut flora, but may also expose it to lethal toxins through the consumption of antimicrobial treatments.

How fluctuations affect species diversity has been a highly contested topic in ecology. The intermediate disturbance hypothesis argues that intermediate intensity and frequency of disturbance maximize species diversity (Connell, 1978; Grime, 1973) because species with high competitive ability dominate at a low level of disturbance while species that adapted to the disturbance dominate at high disturbance (Grime, 1977). This hypothesis is controversial (Fox, 2013) and other relationships between disturbance and species diversity have been reported both empirically and theoretically (Mackey and Currie, 2001; Miller et al., 2011).

Another body of theory that considers how environmental fluctuations can affect species diversity is modern coexistence theory (Chesson, 1994). In modern coexistence theory, spatial and temporal differences in the environment mediate species coexistence when species differ in their preferences for environmental conditions and/or in their response to fluctuations in factors like resources and toxins (Amarasekare, 2019; Chesson, 2000a,b; Letten et al., 2018b; Barabás et al., 2018; Ellner et al., 2019). Resources and toxins have opposite effects on growth rates: consumption of resources by other species decreases the growth rate of a focal species (competition/exploitation) while absorption of toxin by others can increase its growth rate (facilitation). This implies that environmental conditions, especially amounts of resources and toxins, can affect the sign and/or magnitude of species interactions (Hoek et al., 2016; Piccardi et al., 2019; Zuñiga et al., 2019). In turn, how pairs of species in a community interact (i.e., competition or facilitation) affects species diversity and community stability (Mougi and Kondoh, 2012; Coyte et al., 2015). Environmental fluctuations in nutrient and toxin concentrations are therefore expected to affect species interactions, which should then affect community diversity.

Recently, Rodríguez-Verdugo et al. (2019) used theory and experiments to show that the rate of environmental fluctuations affects the coexistence of two species when the environment switches between two carbon sources that promote either exploitation or competition between the species. However, it is unclear whether and how environmental fluctuations in amounts of – rather than types of – resources affect species coexistence and diversity because we do not know how species interactions change *a priori*. More generally, we ask: can

one predict patterns of diversity under fluctuating environments in larger communities composed of more than two species? How do these changes in diversity relate to changes in inter-species interactions? And how do environmental conditions (e.g., resource or toxin concentrations) affect these changes?

To shed light on these questions, we develop a mathematical model to investigate how the rate of environmental fluctuations affects species interactions and diversity. We start with a simple scenario with just two species in an environment that switches between scarce and abundant resource supplies. In addition to resources, our model includes the dynamics of toxins, as we expect them to affect inter-species interactions (Hoek et al., 2016; Piccardi et al., 2019; Zuñiga et al., 2019). Accordingly, the two species can both compete for resources and facilitate each other by absorbing toxic compounds. We focus on the faster grower and ask: (i) How often does this species go extinct due to the presence of a slower-growing species, and (ii) how does such extinction depend on the environmental switching rate and other properties of the environment? For most parameter values, the faster grower's extinction probability increases because of competitive exclusion by the slower grower. To our surprise, we found that this competitive effect peaked at different switching rates depending on environmental toxicity. Second, to verify whether these findings generalize to, and predict the dynamics of larger community dynamics, we simulated communities of up to 10 species and found a similar pattern: beta diversity was highest at different switching rates in different environments. Although various relationships between disturbance and diversity have been previously reported (Mackey and Currie, 2001; Miller et al., 2011), our model associates the strength of competition between two species with the loss of beta diversity in a larger community in a fluctuating environment. In other words, to estimate how beta diversity changes over the environmental switching rate, it may be sufficient to analyze the sign and strength of interactions between two representative species under those same conditions.

2 Model

In this paper, we analyze how environmental switching rate ν affects species interactions and diversity in a chemostat model. For simplicity, we assume symmetric random switching (but see Taitelbaum et al. (2020) for asymmetric, random and periodic switching). This model combines two sources of noise: birth and death events occur randomly yielding demographic noise, while the environment randomly switches from being harsh to mild and vice versa and drives the population size (Wienand et al., 2017, 2018; West and Mobilia, 2020; Taitelbaum et al., 2020). When the environment becomes harsh (e.g., abundant toxins or scarce resources), the population shrinks and demographic noise can lead to extinction. As in previous work, a distinctive feature of this model is therefore the coupling of demographic and environmental noise: environmental switching changes the population size, which in turn modulates demographic fluctuations, which results in feedback loops. Here, we implement environmental switching by modeling time-varying resource and/or toxin supplies, as we are interested in how these environmental conditions mediate species interactions and diversity.

Our model includes the dynamics of the amount r_i of resource i ($i = 1, \ldots, N/2$, where N is an even number) that allows all species to grow, the amount t_j of toxic compound j ($j = 1, \ldots, N/2$) that kills all species, and the

abundance s_k of species k ($k = 1, \ldots, N$). When $N = 2$ species, we recapitulate the environmentally mediated species interactions shown in the model of Piccardi et al. (2019), where species affect each other positively in toxic environments, with increasing competition in more benign environments. The dynamics are modelled in terms of a multivariate continuous-time birth-and-death process (see Novozhilov et al. (2006); Allen (2010) for example) defined by the following "birth" and "death" reactions:

$$r_i \xrightarrow{\tau^+_{r_i}} r_i + 1, \tag{1a}$$

$$r_i \xrightarrow{\tau^-_{r_i}} r_i - 1, \tag{1b}$$

$$t_j \xrightarrow{\tau^+_{t_j}} t_j + 1, \tag{1c}$$

$$t_j \xrightarrow{\tau^-_{t_j}} t_j - 1, \tag{1d}$$

$$s_k \xrightarrow{\tau^+_{s_k}} s_k + 1, \tag{1e}$$

$$s_k \xrightarrow{\tau^-_{s_k}} s_k - 1, \tag{1f}$$

occurring with transition rates:

$$\tau^+_{r_i} = \alpha R_i\left(\xi\right), \tag{2a}$$

$$\tau^-_{r_i} = \sum_{k=1}^{N} \frac{\mu_{ik}}{Y^r_{ik}} \frac{r_i}{r_i + K^r_{ik}} s_k + \alpha r_i, \tag{2b}$$

$$\tau^+_{t_j} = \alpha T_j\left(\xi\right), \tag{2c}$$

$$\tau^-_{t_j} = \sum_{k=1}^{N} \frac{\delta_{jk}}{Y^t_{jk}} \frac{t_j}{t_j + K^t_{jk}} s_k + \alpha t_j, \tag{2d}$$

$$\tau^+_{s_k} = \sum_{i=1}^{N/2} \mu_{ik} \frac{r_i}{r_i + K^r_{ik}} s_k, \tag{2e}$$

$$\tau^-_{s_k} = \sum_{j=1}^{N/2} \delta_{jk} \frac{t_j}{t_j + K^t_{jk}} s_k + \alpha s_j, \tag{2f}$$

where α is the dilution rate of the chemostat, $\xi = \pm 1$ (see below) represents changing environmental conditions in terms of in-flowing resource and/or toxin concentration, $R_i(\xi)$ ($T_j(\xi)$) is resource i's (toxin j's) supply under the environmental condition ξ, Y^r_{ik} (Y^t_{jk}) is species k's biomass yield for resource i (toxin j), μ_{ik} is the maximum growth rate of species k by resource i, δ_{jk} is the maximum death rate of species k by toxin j (species k's sensitivity to toxin j), and K^r_{ik} (K^t_{jk}) is the amount of resource i (toxin j) that gives the half-maximum growth (death) rate of species k. In this model, we assume that growth and death rates depend on the amounts of resource and toxin in Monod function forms, respectively, and that the effects are additive.

Environmental switching changes resource and/or toxin supplies at rate ν according to

$$\xi \xrightarrow{\nu} -\xi, \tag{3}$$

where $\xi \in \{-1, +1\}$ is a coloured dichotomous (telegraph) noise assumed to be symmetric and stationary (Bena, 2006; Horsthemke and Lefever, 2006). Here, the mean of $\xi(t)$ is therefore always zero and its finite correlation time is $1/\nu$. One can imagine three environmental switching scenarios, where either or both resource and toxin supplies change (Table 1). In the main text, we analyze only scenario 1 where only resource supplies switch, but see Appendix 4 for the remaining scenarios. When environmental switching affects the resource supply R_i, it switches between abundant and scarce:

$$R_i(\xi) = \begin{cases} R_i^+ & \xi = 1 \text{ (abundant)} \\ R_i^- & \xi = -1 \text{ (scarce)} \end{cases} \quad \text{s.t. } R_i^+ > R_i^- > 0, \forall i. \tag{4}$$

It is clear that (2a)-(4) define a multivariate birth-and-death process *coupled* with environmental switching. As environmental switching does not affect toxin supply in this scenario, the mean amount of toxins is supplied $\langle T_j \rangle$, where $\langle \cdot \rangle$ represents the mean of abundant and scarce supplies of a focal resource or toxin (e.g., $\langle T_j \rangle \equiv \left(T_j^+ + T_j^-\right)/2$ such that $T_j^+ > T_j^- > 0, \forall j$).

Note that when demographic noise is ignored, the sole source of randomness stems from the dichotomous Markov noise, which clearly results in the waiting time between two environmental switches to be exponentially distributed with a mean $1/\nu$ (Bena, 2006). In the joint presence of demographic noise and environmental switching, see, e.g., (Hufton et al., 2016; West et al., 2018), the waiting time approximately follows the exponential distribution with mean $1/\nu$, with the larger the switching rate the shorter the sojourn in either of the environmental states.

The master equation for this model is defined by combining the dynamics of amount of resources and toxins, abundances of species, and environmental switching (Eqs (1a) - (3)):

$$\begin{aligned} \dot{P}\left(\vec{r}, \vec{t}, \vec{s}, \xi\right) = & \sum_{i=1}^{N/2} \left(\mathbb{E}_{r_i}^- - 1\right) \left\{\tau_{r_i}^+ P\left(\vec{r}, \vec{t}, \vec{s}, \xi\right)\right\} \\ & + \sum_{i=1}^{N/2} \left(\mathbb{E}_{r_i}^+ - 1\right) \left\{\tau_{r_i}^- P\left(\vec{r}, \vec{t}, \vec{s}, \xi\right)\right\} \\ & + \sum_{j=1}^{N/2} \left(\mathbb{E}_{t_j}^- - 1\right) \left\{\tau_{t_j}^+ P\left(\vec{r}, \vec{t}, \vec{s}, \xi\right)\right\} \\ & + \sum_{j=1}^{N/2} \left(\mathbb{E}_{t_j}^+ - 1\right) \left\{\tau_{t_j}^- P\left(\vec{r}, \vec{t}, \vec{s}, \xi\right)\right\} \\ & + \sum_{k=1}^{N} \left(\mathbb{E}_{s_k}^- - 1\right) \left\{\tau_{s_k}^+ P\left(\vec{r}, \vec{t}, \vec{s}, \xi\right)\right\} \\ & + \sum_{k=1}^{N} \left(\mathbb{E}_{s_k}^+ - 1\right) \left\{\tau_{s_k}^- P\left(\vec{r}, \vec{t}, \vec{s}, \xi\right)\right\} \\ & + \nu \left\{P\left(\vec{r}, \vec{t}, \vec{s}, -\xi\right) - P\left(\vec{r}, \vec{t}, \vec{s}, \xi\right)\right\} \end{aligned} \tag{5}$$

where $P\left(\vec{r}, \vec{t}, \vec{s}, \xi\right)$ represents the probability density of $\vec{r} = (r_i)$, $\vec{t} = (t_j)$, $\vec{s} = (s_k)$, and ξ, the dot denotes the

time derivative, and $\mathbb{E}^{\pm}_{r_i}$ is a shift operator such that

$$\mathbb{E}^{\pm}_{r_i} P\left(\vec{r}, \vec{t}, \vec{s}, \xi\right) = P\left(r_1, \ldots, r_i \pm 1, \ldots, r_{N/2}, \vec{t}, \vec{s}, \xi\right), \tag{6}$$

and $\mathbb{E}^{\pm}_{t_j}$ and $\mathbb{E}^{\pm}_{s_k}$ are the equivalent shift operators for t_j and s_k, respectively. The last line on the right-hand-side of (5) accounts for the random switching reaction (3). The model given by Eq. (5) was implemented using the Gillespie algorithm (Gillespie, 1977) until, after a sufficiently large time T_{end}, the population size distribution converges to a quasi-stationary distribution (i.e., where distributions of species abundances appear to be stationary for a long time; the real equilibrium state corresponding to the extinction of all species being practically unobservable). In two species scenarios, either or both two species go extinct before time T_{end} in most cases (see Fig. 4 column C.). For details on parameter values and the simulations, see Appendix 2. A schematic illustration of this model with $N = 2$ is summarized in Fig. 1.

2.1 Evaluating species interactions

We begin by analyzing interactions between two species ($N = 2$) where the sign and magnitude of species interactions can change. We used parameter values such that species 1 always outcompetes species 2 in a deterministic and fixed environment setting (i.e., species 1 grows faster than species 2, see Appendix 1 for analysis and Table A.1 for exact parameter values) to clarify the effects of demographic noise. Under demographic noise coupled with environmental switching, either of the two species or both species tend to go extinct. As a proxy for interactions, we focus on the net effect of species 2 on species 1, which is defined by the extinction probability of species 1 in mono-culture minus that in co-culture with species 2:

$$\Delta P\left(s_1(T_{end}) = 0\right) \equiv P\left(s_1(T_{end}) = 0; s_2(0) = 0\right) - P\left(s_1(T_{end}) = 0; s_2(0) > 0\right). \tag{7}$$

If $\Delta P\left(s_1(T_{end}) = 0\right)$ is < -0.01, we consider that species 2 increases the extinction probability of species 1 (negative effect), whereas $\Delta P\left(s_1(T_{end}) = 0\right) > 0.01$ implies that species 2 has a positive effect on species 1. We ignore small values of $|\Delta P\left(s_1(T_{end}) = 0\right)|$, as they are biologically meaningless and may be due to the finite number of simulations.

In the analysis of species diversity (see below) with $N = 2$, we also analyzed the species interactions in 100 pairs of species that differ in $\mu_{ik}, K^r_{ik}, \delta_{jk}$, and K^t_{jk} in the presence of demographic noise and environmental switching. Since pairs of species may coexist depending on their parameter values in the diversity analysis, species 1 (or 2) is the one that has larger (or smaller) population size than the other in the absence of any noise. If both species go extinct in the absence of noise, species 1 is chosen randomly.

2.2 Evaluating species diversity

To explore how species diversity changes over switching rates, we ran simulations at different community sizes ranging from $N = 2$ to $N = 10$ and different mean toxin sensitivities, from $\bar{\delta} = 0.1$ to $\bar{\delta} = 1$. For each

condition (one N and one $\bar{\delta}$), we sampled 100 sets of parameters $\mu_{ik}, K^r_{ik}, \delta_{jk}$, and K^t_{jk}, which represented 100 meta-communities composed of N species whose differences were reflected in the parameter values. Each meta-community had 100 independent communities (no inter-community migration and independent environmental switching) with equal initial species abundances. In short, we replicated 100 simulations for each of 100 sets of parameter values, and we had in total 10,000 simulations for each combination of community size, mean toxin sensitivity, and switching rate.

Because demographic noise and environmental switching affect species composition, we investigated the heterogeneity of communities at the end of each simulation run. We measured beta diversity (Jost, 2007; Chao et al., 2012) of each meta-community and species richness (number of surviving species) for each community at a quasi-stationary state (T_{end}):

$$ {}^1D_\beta\left(T_{end}\right) \equiv \frac{{}^1D_\gamma\left(T_{end}\right)}{{}^1D_\alpha\left(T_{end}\right)}, \tag{8} $$

with alpha and gamma diversities defined as below:

$$ {}^1D_\alpha\left(T_{end}\right) \equiv \exp\left(-\sum_{l=1}^{100}\sum_{k=1}^{N} w_l p_{lk}\left(T_{end}\right)\ln p_{ln}\left(T_{end}\right)\right), \tag{9} $$

$$ {}^1D_\gamma\left(T_{end}\right) \equiv \exp\left(-\sum_{k=1}^{N} \bar{p}_k \ln \bar{p}_k\left(T_{end}\right)\right). \tag{10} $$

w_l is a weight for community l calculated by size of community l (sum of species abundances in community l relative to the sum of community sizes over l), p_{lk} is the relative abundance of species k in community l (i.e., in community l, $p_{lk}\left(T_{end}\right) = s_k\left(T_{end}\right) / \sum_k s_k\left(T_{end}\right)$), and $\bar{p}_k = \sum_l w_l p_{lk}$ is the mean relative abundance of species k among communities $l = 1, \ldots, 100$. If all species go extinct in community l, it does not affect alpha, beta and gamma diversities as $w_l = 0$. If all species go extinct in all communities, beta diversity becomes ${}^1D_\beta\left(T_{end}\right) = 1$. For more detail, see Appendix 2.

2.3 Statistical analysis

Statistical analysis was performed with Python 3.7.6 and Scipy 1.4.1. For statistical tests of Spearman's rank-order correlation, scipy.stats.spearmanr was used.

3 Results

3.1 Toxin sensitivity changes how switching rate affects species interactions

Our aim is to investigate how species interactions and diversity change over the environmental switching rate. Rather than measuring interactions through the effect of each species on the other's biomass, we focus on a fast-growing species (that we call species 1) and analyze how its extinction probability is affected by the presence of a second slower-growing species (species 2). Our reasoning here is that in the absence of noise, species 1

should always out-compete species 2, so measuring any deviation from this outcome allows us to quantify the effect of coupled demographic noise and environmental fluctuations. We explored how this proxy for species interactions was affected by different environmental switching rates as well as different toxin sensitivities, which we varied simultaneously for both species, such that the species were always equally sensitive to the toxin.

When both species were highly sensitive to the toxin (large δ), species 2 has a positive effect on species 1. This occurs because species 2 also degrades the toxin, which outweighs the competition for nutrients (Piccardi et al., 2019). However, for most parameter values in Fig. 2A, species 2 has a negative effect on species 1 by increasing its extinction probability. We therefore focus on competitive interactions (i.e., $\Delta P\left(s_1(T_{end})=0\right)<0$) for the remainder of the main part of the study and consider positive interactions in Appendix 5.

As we varied the switching rate, we observed that the strength of the competitive effect was highly dependent on the toxin sensitivity δ of the two species: monotonically increasing, monotonically decreasing, or non-monotonically changing with a minimum or maximum value at an intermediate switching rate (Fig. 2B). How our system behaves under the two extreme switching rates becomes clear if one considers what happens in the absence of environmental switching (Fig. A.3). At very low rate $\nu \to 0$, there are almost no switches: the environment remains either poor or rich in nutrient (probability 1/2) and microbes are as likely to experience either scarce or abundant resources from $t=0$ until $t=T_{end}$. The outcome at this switching rate therefore corresponds to the mean outcome of those two environments. On the other hand, a very fast environmental switching rate ($\nu \to \infty$) corresponds to a scenario where the resource supply is at mean concentration (environmental noise self averages, see, e.g.,Wienand et al. (2017, 2018); West and Mobilia (2020); Taitelbaum et al. (2020)). How the strength of competition varies at an intermediate switching rate is, however, less intuitive. We explore this next.

3.2 Competitive exclusion explains negative species interactions

To better understand the unexpected changes in the effect of species 2 on species 1 (Fig. 2B), we analyse our proxy for species interactions in more detail. $\Delta P\left(s_1(T_{end})=0\right)$ represents the difference between the probability of species 1 going extinct in mono-culture ($P\left(s_1(T_{end})=0; s_2(0)=0\right)$) versus in co-culture with species 2 ($P\left(s_1(T_{end})=0; s_2(0)>0\right)$) (Eq. 7). By decomposing the co-culture component into two probabilities depending on whether species 2 persists or not and rearranging the equation, we obtain:

$$\begin{aligned}\Delta P\left(s_1(T_{end})=0\right) = &-\underbrace{P\left(s_1(T_{end})=0, s_2(T_{end})>0; s_2(0)>0\right)}_{\text{competitive exclusion}} \\ &+\left\{\underbrace{P\left(s_1(T_{end})=0; s_2(0)=0\right)}_{\text{sp 1 goes extinct in mono-culture}} - \underbrace{P\left(s_1(T_{end})=0, s_2(T_{end})=0; s_2(0)>0\right)}_{\text{both species go extinct}}\right\}.\end{aligned} \tag{11}$$

The first line of Eq (11) represents the probability that species 2 excludes species 1 and survives (competitive exclusion), while the second line is species 1's extinction probability in mono-culture minus the probability of

both species going extinct.

Fig. A.2 shows that the overall interaction strength is not affected much by the second line of Eq (11), and that the competitive exclusion probability explains the variation in species interaction strength in most cases (compare Fig. 2A and C). Intuitively, this is because under the environmental conditions where both species are likely to go extinct (i.e., small resource supplies and high toxin sensitivity), species 1 is also likely to go extinct in mono-culture, resulting in a small magnitude of the second line of Eq (11). For this reason, the competitive exclusion probability changes similarly to the effect of species 2 on species 1 over environmental switching rates and toxin sensitivities (Fig. 2C). In other words, we can assume that the second line of Eq (11) is negligible and focus instead on the competitive exclusion probability.

3.3 Competitive exclusion explains non-monotonic changes in species interactions

Following the logic outlined above, we now use the competitive exclusion probability to investigate why the strength of negative interactions changes over the switching rate in various ways, depending on toxin sensitivity.

In the absence of environmental switching, the competitive exclusion probability is uni-modal over toxin sensitivity δ, regardless of the resource supply (Fig. 3A). As a reminder, competitive exclusion implies the extinction of species 1 and the survival of species 2. Since toxin sensitivity is identical for both species, when toxin sensitivity is too high, both species are likely to go extinct (Fig. A.4), which does not count as competitive exclusion. Instead, competitive exclusion is most likely at lower toxin sensitivities whose value depends on the amount of resource supply: when more resources are supplied, the peak moves to a higher toxin sensitivity because species are more likely to survive (Fig. 3A). Hereafter, we refer to the toxin sensitivity that maximizes the competitive exclusion probability in the absence of environmental switching as the "critical toxin sensitivity".

This analysis clarifies what happens at the two extreme switching rates. At a very slow switching rate ($\nu \to 0$), the environment remains for a long time with either scarce or abundant resources. Accordingly, competitive exclusion has two peaks over the toxin sensitivity (at $\delta = 0.1$ and 0.8 in Figs. 2C and D) corresponding to the critical toxin sensitivities under the scarce and abundant resource supplies in Fig. 3A, respectively. On the other hand, at very fast switching rates ($\nu \to \infty$), where resources remain at mean abundance, competitive exclusion has one peak (at $\delta = 0.4$ in Figs. 2C and D) corresponding to the critical toxin sensitivity under the mean resource supply in Fig. 3A. In sum, the form of the competitive exclusion probability in Fig. 2C changes from bi-modal to uni-modal by increasing the switching rate.

The non-monotonic change of competitive exclusion probability over the switching rate can happen at toxin sensitivities between the critical toxin sensitivities under scarce (or abundant) and mean resource supplies (Fig. 2C). This phenomenon can be explained by considering that the landscape of competitive exclusion depicted in Fig. 2C contains two "mountain ranges". The first "mountain range" includes two peaks corresponding to the critical toxin sensitivities under the scarce and mean resource supplies ($\delta = 0.1, 0.4$, respectively). By increasing environmental switching from a very slow rate, the peak at $\delta = 0.1$ converges to the peak at $\delta = 0.4$ (Fig. 2D). The second "mountain range" consists of the peak corresponding to the critical toxin sensitivity under the

abundant resource supply ($\delta = 0.8$). This peak vanishes by increasing the switching rate (Fig. 2D).

At toxin sensitivities between critical values under scarce and mean resource supplies ($\delta = 0.2, 0.3$), the competitive exclusion probability changes in a humped shape over the switching rate (species interactions change in a U shape, see Fig. 2B). This is because an intermediate switching rate has a peak of competitive exclusion probability belonging to the first mountain range. When the toxin sensitivity is $\delta = 0.6$, the environmental switching rate also non-monotonically affects the competitive exclusion probability, but for a different reason. Toxin sensitivities between the critical values under mean and abundant resource supplies can have a "valley" over the switching rate: at such toxin sensitivities, competitive exclusion probability changes in a U shape over the switching rate (species interactions change in a humped shape, see Fig. 2B). At toxin sensitivities larger than the critical value under the abundant resource supply, competitive exclusion probability is very small and does not change non-monotonically over the switching rate because both species frequently go extinct (Fig A.4).

3.4 Non-monotonic changes in species interactions happen under different scenarios of environmental differences

We have shown that using a given set of parameters, the rugged landscape shown in Fig. 2C causes competition to either increase, decrease or vary non-monotonically across switching rates, depending on toxin sensitivity. We next explore the generality of this finding and ask whether it will hold under different scenarios. In the appendix, we explore scenarios where (i) switching occurs in toxin rather than resource supplies, where (ii) both resource and toxin supplies switch (Table 1, see Appendix 4), or where (iii) we change the amounts of scarce and abundant resource supplies (Appendix 5).

In all these scenarios, the landscapes of competitive exclusion probability also contain two "mountain ranges" (Figs. A.5, A.7), leading, as before, to a variety of patterns as switching rates and toxin sensitivities change. In each scenario, the distances between the three critical toxin sensitivities (mild, mean and harsh, e.g. black arrow in Fig. 3A) change (see Table A.2). Do these distances predict the shape of the landscape and the probability of observing non-monotonic behavior? In Table A.2 and Fig. 3B we show that the distance between critical sensitivities under harsh and mean environments (i.e., very fast environmental switching) correlates positively with the likelihood of observing non-monotonic effects of the switching rate on competition (Fig. 3B, black circles; Spearman's $\rho = 0.77$, P-value: 0.043), but no significant correlation was found with the distance between the critical toxin sensitivities under the mean and mild, or the harsh and mild environments (Fig. 3B, grey diamonds and cross marks; Spearman's $\rho = -0.22$, P-value: 0.64, and $\rho = 0.42$, P-value: 0.35, respectively). These differences can be explained by changes in the shape of the landscape (see subsection 3.3). In sum, we find non-monotonic behavior under many different scenarios, with no easily observable pattern for when they occur. Overall, this makes it challenging to predict how the strength of interspecific interactions will change over environmental switching rates.

3.5 Beta diversity changes similarly to competitive exclusion

In the previous sections, we have focused on interactions between two species and the conditions under which they may drive each other extinct. Ultimately, however, our interest is to predict how species diversity is affected by the environment in communities comprised of tens, hundreds or even thousands of species. In this section, we ask whether the same rules that we have uncovered between two species apply for larger communities of up to 10 species. Will the diversity of a community similarly depend on environmental switching rates and toxin sensitivities?

We address this question by extending our model to simulate communities of between 2 and 10 species. Simulating larger communities with this model would be too computationally expensive. As our model includes stochastic environmental switching and demographic noise, we ran 10'000 simulations for each community size and for each of 5 different mean toxin sensitivities (here species in a community could differ in their toxin sensitivity) ranging from $\bar{\delta} = 0.1$ to $\bar{\delta} = 1$ (see Methods). At the end of each simulation run, we measured the beta diversity and species richness (number of surviving species). These 10'000 (100×100) simulations were composed of 100 replicate runs for one of 100 randomly sampled sets of parameter values (see Methods).

In two-species communities, beta diversity changes over the environmental switching rate similarly to the competitive exclusion probability for four out of five mean toxin sensitivities (columns A and B in Fig. 4): both monotonically decrease (mean toxin sensitivity $\bar{\delta} = 0.1$ or 1.0), or non-monotonically change with maximum ($\bar{\delta} = 0.2$) or minimum ($\bar{\delta} = 0.6$) values at intermediate switching rates. At one mean toxin sensitivity $\bar{\delta} = 0.4$, the patterns of competitive exclusion and beta diversity over the switching rate do not match. Our measure of final species richness (column C in Fig. 4) shows that at low switching rates and $\bar{\delta} = 0.4$, both species can sometimes co-exist, which keeps beta-diversity high. Although two species can also coexist when $\bar{\delta} = 0.1$ or 0.2, the probability of coexistence changes over the switching rate similarly to the competitive exclusion probability, leading to similar patterns in both measures.

We next increase the number of species in community to 10 (Figs. A.10 and A.11) to see whether the same patterns of beta diversity are observed. The similarity remains in 10-species communities (columns D and E in Fig. 4). Although variation in species richness increases beta diversity, the inverse is not true: beta diversity can be large when species richness is likely to be one (see $\bar{\delta} = 0.4$ and 0.6 at switching rate larger than 10^1 in D and E columns in Fig. 4). In such cases, different species fixate in each simulation by competitive exclusion. In sum, estimating the competitive exclusion probability in two species in a given environment is a good predictor for the beta diversity of larger communities under those same environmental conditions.

4 Discussion

Understanding how species diversity in microbial communities arises and is maintained is a central question in microbial ecology and evolution. Diversity is affected by biotic interactions between species, but also by abiotic properties of the environment, such as its harshness (availability of nutrients and/or toxicity), and how conditions fluctuate over time. Here we have used a mathematical model to explore the relationship between

these three factors and how they affect the diversity of small communities.

Our study is centred on two main findings. First, we show that the rate at which resource abundance fluctuates in the environment changes the strength of negative interactions (competition) – quantified as the ability of a slower-growing species to drive a fast-growing one extinct. However, these changes depend strongly on how toxic the environment is for both species. As the switching rate increases, competition can monotonically increase, monotonically decrease, or change non-monotonically (Fig. 2B), depending on toxin sensitivity. These negative interactions mostly manifest themselves as competitive exclusion, rather than the extinction of both species (Figs. 2C and A.2). By calculating the critical toxin sensitivities that maximize competitive exclusion in the absence of environmental switching, one can predict how the switching rate will affect the strength of competition at a given toxin sensitivity. Our second main finding is that studying changes in the probability of two species competitively excluding one another is a good indicator for how the beta diversity of a community composed of up to 10 species will change with environmental switching (Fig. 4).

This brings us to a hypothesis that has been debated at length in ecology: the intermediate disturbance hypothesis (Connell, 1978; Grime, 1973), which states that intermediate intensity and frequency of disturbance maximize species diversity. Fox (2013) argues that the intermediate disturbance hypothesis should be abandoned because many examples disagree with it (Mackey and Currie, 2001; Miller et al., 2011). In our model, fluctuations in resource and toxin concentrations can be regarded as disturbances. In agreement with Mackey and Currie (2001) and Miller et al. (2011) then, an intermediate intensity (i.e., toxin sensitivity) or disturbance frequency (environmental switching rate) does not always maximize beta diversity: our analysis shows that intermediate frequencies of disturbance maximize beta diversity only when mean toxin sensitivity is within a certain range. Mean toxin sensitivities at the two thresholds of this range show that beta diversity monotonically decreases or increases over the switching rate. These thresholds depend on scenarios of environmental switching and amounts of resource supplies because these parameters change probability of competitive exclusion (see Appendix 4 and Appendix 5). High diversity at intermediate disturbances is then a consequence of a change in environmental conditions and not expected to apply generally.

The relationship between environmental fluctuations and species diversity is also an important question in modern coexistence theory, which predicts that fluctuations will affect species coexistence by changing species growth rates when rare (Chesson, 2000a,b; Barabás et al., 2018; Ellner et al., 2019; Letten et al., 2018a). Compared to the approach taken in this study – where we ask how many and which species persist at the end of a long but fixed time frame (i.e., for a quasi-stationary distribution, Fig. 4) – modern coexistence theory allows one to analyze whether or for how long a set of species will all coexist (Schreiber et al., 2020). An interesting future direction would be to apply modern coexistence theory to investigate how environmental fluctuation rates and toxin sensitivities affect the duration of all-species coexistence. This approach would help to propose biological mechanisms behind species coexistence in our setup.

Of course, our model makes some simplifying assumptions and has some limitations. First, we used arbitrary time units, which in practice can be considered to be hours, corresponding to typical bacterial growth rates in relevant experiments (Novick and Szilard, 1950; Lin et al., 2002; Zhao and Lin, 2003). This implies that species

interactions and beta diversity will vary when environmental switching ranges from hourly ($\nu = 10^0$) to about once every four days ($\nu = 10^{-2}$) on average, which is shorter than in some experimental studies (Benneir and Lenski, 1999; Rodríguez-Verdugo et al., 2019; Chen and Zhang, 2020) but not impractical. That said, under this assumption, changing an hourly to a monthly scale, for example, would have different effects on ecological dynamics. Second, the switching rate is assumed to be symmetric between abundant and scarce resources (and/or toxin supplies, see Appendix 4). One may include more than two environmental conditions or assume asymmetric environmental switching, as in work by Taitelbaum et al. (2020), who show that asymmetric switching can non-trivially change the effects of environmental switching. Third, our model focuses on competitive exclusion but other types of interactions can also affect diversity (Rodríguez-Verdugo et al., 2019). Positive interactions between pairs of species (e.g., cross-feeding), for example, might increase alpha and gamma diversities, because such interactions enable species to coexist (Sun et al., 2019). This could result in an increase in beta diversity because the extinction of one species by demographic noise, for example, increases its partner species' extinction probability. Finally, our community analysis considers up to ten microbial species, which is orders of magnitude below the size of natural microbial communities, according to genomic sampling (Gans, 2005; Roesch et al., 2007). However, it may also be reasonable to assume that species live in structured environments where they cannot possibly interact with more than a handful of other genotypes (Tecon et al., 2019). This suggests that a 10-species community may already be biologically meaningful.

In conclusion, the time scale of environmental switching affects the strength of species interactions, which results in changing beta diversity via competitive exclusion. In addition, how species interactions and beta diversity change with respect to the environmental switching rate varies and depends on how the species are sensitive species to the environmental toxicity. This may be one mechanism which explains why the intermediate disturbance hypothesis does not always hold. The variety with which species interactions and beta diversity change over the switching rate means that it will be very difficult to predict how a given ecosystem, such as the gut microbiome, will behave under environmental fluctuations. Nevertheless, the similarity between how competitive exclusion plays out between two species and beta diversity at the community level means that analysing how the former changes over switching rates (as in Rodríguez-Verdugo et al. (2019), for example) may be sufficient to predict the latter. More generally, our study, along with others (Mackey and Currie, 2001; Miller et al., 2011) show that predicting how the environment shapes diversity in ecology remains a challenging problem. Nevertheless, models like the one presented here can help to disentangle the environmental factors contributing to species diversity.

Acknowledgement

S.S. is funded by University of Lausanne and Nakajima foundation. S.M. is funded by European Research Council Starting Grant 715097 and the University of Lausanne. The authors declare no conflict of interest.

Data accessibility

The programming codes and csv files for this manuscript are available in Github.

References

Allen, L. J. S. *An Introduction to Stochastic Processes with Applications to Biology*. Chapman and Hall/CRC, New York, 2nd edition, 2010. ISBN 9780429184604. doi: 10.1201/b12537. URL https://www.taylorfrancis.com/books/9781439894682.

Amarasekare, P. The evolution of coexistence theory. *Theoretical Population Biology*, 133:49–51, 2019. ISSN 10960325. doi: 10.1016/j.tpb.2019.09.005. URL https://doi.org/10.1016/j.tpb.2019.09.005.

Barabás, G., D'Andrea, R., and Stump, S. M. Chesson's coexistence theory. *Ecological Monographs*, 0(0):1–27, 2018. ISSN 00129615. doi: 10.1002/ecm.1302. URL http://doi.wiley.com/10.1002/ecm.1302.

Bena, I. Dichotomous Markov noise: Exact results for out-of-equilibrium systems. A review. *International Journal of Modern Physics B*, 20(20):2825–2888, 6 2006. ISSN 02179792. doi: 10.1142/S0217979206034881. URL http://arxiv.org/abs/cond-mat/0606116.

Benneir, A. F. and Lenski, R. E. Experimental evolution and its role in evolutionary physiology. *American Zoologist*, 39(2):346–362, 1999. ISSN 00031569. doi: 10.1093/icb/39.2.346.

Chao, A., Chiu, C. H., Hsieh, T. C., and Inouye, B. D. Proposing a resolution to debates on diversity partitioning. *Ecology*, 93(9):2037–2051, 9 2012. ISSN 00129658. doi: 10.1890/11-1817.1. URL http://doi.wiley.com/10.1890/11-1817.1.

Chen, P. and Zhang, J. Antagonistic pleiotropy conceals molecular adaptations in changing environments. *Nature Ecology & Evolution*, 2 2020. ISSN 2397-334X. doi: 10.1038/s41559-020-1107-8. URL http://www.nature.com/articles/s41559-020-1107-8.

Chesson, P. Multispecies Competition in Variable Environments. *Theoretical Population Biology*, 45:227–276, 1994.

Chesson, P. Mechanisms of Maintenance of Species Diversity. *Annual Review of Ecology and Systematics*, 31(1):343–366, 11 2000a. ISSN 0066-4162. doi: 10.1146/annurev.ecolsys.31.1.343. URL http://www.annualreviews.org/doi/10.1146/annurev.ecolsys.31.1.343.

Chesson, P. General theory of competitive coexistence in spatially-varying environments. *Theoretical Population Biology*, 58(3):211–237, 2000b. ISSN 00405809. doi: 10.1006/tpbi.2000.1486.

Cignarella, F., Cantoni, C., Ghezzi, L., Salter, A., Dorsett, Y., Chen, L., Phillips, D., Weinstock, G. M., Fontana, L., Cross, A. H., Zhou, Y., and Piccio, L. Intermittent Fasting Confers Protection in CNS Autoimmunity by Altering the Gut Microbiota. *Cell Metabolism*, 27(6):1222–1235, 2018. ISSN 19327420. doi: 10.1016/j.cmet.2018.05.006. URL https://doi.org/10.1016/j.cmet.2018.05.006.

Connell, J. H. Diversity in Tropical Rain Forests and Coral Reefs. *Science*, 199(4335):1302–1309, 1978.

Coyte, K. Z., Schluter, J., and Foster, K. R. The ecology of the microbiome: Networks, competition, and stability. *Science*, 350(6261):663–666, 2015. ISSN 0036-8075. doi: 10.1126/science.aad2602. URL http://www.sciencemag.org/cgi/doi/10.1126/science.aad2602.

Davenport, E. R., Mizrahi-Man, O., Michelini, K., Barreiro, L. B., Ober, C., and Gilad, Y. Seasonal variation in human gut microbiome composition. *PLoS ONE*, 9(3), 2014. ISSN 19326203. doi: 10.1371/journal.pone.0090731.

Ellner, S. P., Snyder, R. E., Adler, P. B., and Hooker, G. An expanded modern coexistence theory for empirical applications. *Ecology Letters*, 22(1):3–18, 1 2019. ISSN 1461-023X. doi: 10.1111/ele.13159. URL https://onlinelibrary.wiley.com/doi/abs/10.1111/ele.13159.

Fox, J. W. The intermediate disturbance hypothesis should be abandoned. *Trends in Ecology & Evolution*, 28(2):86–92, 2 2013. ISSN 01695347. doi: 10.1016/j.tree.2012.08.014. URL https://linkinghub.elsevier.com/retrieve/pii/S0169534712002091.

Gans, J. Computational Improvements Reveal Great Bacterial Diversity and High Metal Toxicity in Soil. *Science*, 309(5739):1387–1390, 8 2005. ISSN 0036-8075. doi: 10.1126/science.1112665. URL https://www.sciencemag.org/lookup/doi/10.1126/science.1112665.

Gillespie, D. T. Exact stochastic simulation of coupled chemical reactions. *Journal of Physical Chemistry*, 81(25):2340–2361, 1977. ISSN 00223654. doi: 10.1021/j100540a008.

Grime, J. P. Competitive Exclusion in Herbaceous Vegetation. *Nature*, 242(5396):344–347, 3 1973. ISSN 0028-0836. doi: 10.1038/242344a0. URL http://www.nature.com/doifinder/10.1038/242344a0.

Grime, J. P. Evidence for the Existence of Three Primary Strategies in Plants and Its Relevance to Ecological and Evolutionary Theory. *The American Naturalist*, 111(982):1169–1194, 1977. ISSN 0003-0147. doi: 10.1086/283244.

Hengge-Aronis, R. Survival of hunger and stress: The role of rpoS in early stationary phase gene regulation in E. coli. *Cell*, 72(2):165–168, 1 1993. ISSN 00928674. doi: 10.1016/0092-8674(93)90655-A. URL https://linkinghub.elsevier.com/retrieve/pii/009286749390655A.

Himeoka, Y. and Mitarai, N. Dynamics of bacterial populations under the feast-famine cycles. *arXiv*, pages 1–39, 10 2019. URL http://arxiv.org/abs/1910.05673.

Hoek, T. A., Axelrod, K., Biancalani, T., Yurtsev, E. A., Liu, J., and Gore, J. Resource Availability Modulates the Cooperative and Competitive Nature of a Microbial Cross-Feeding Mutualism. *PLOS Biology*, 14(8):e1002540, 8 2016. ISSN 1545-7885. doi: 10.1371/journal.pbio.1002540. URL http://dx.plos.org/10.1371/journal.pbio.1002540.

Horsthemke, W. and Lefever, R. *Noise-Induced Transitions*, volume 15 of *Springer Series in Synergetics*. Springer Berlin Heidelberg, 2nd edition, 4 2006. ISBN 978-3-540-11359-1. doi: 10.1007/3-540-36852-3. URL http://link.springer.com/10.1007/3-540-36852-3.

Hufton, P. G., Lin, Y. T., Galla, T., and McKane, A. J. Intrinsic noise in systems with switching environments. *Physical Review E*, 93(5):1–13, 2016. ISSN 24700053. doi: 10.1103/PhysRevE.93.052119.

Jost, L. PARTITIONING DIVERSITY INTO INDEPENDENT ALPHA AND BETA COMPONENTS. *Ecology*, 88(10):2427–2439, 10 2007. ISSN 0012-9658. doi: 10.1890/06-1736.1. URL http://doi.wiley.com/10.1890/06-1736.1.

Letten, A. D., Dhami, M. K., Ke, P. J., and Fukami, T. Species coexistence through simultaneous fluctuation-dependent mechanisms. *Proceedings of the National Academy of Sciences of the United States of America*, 115(26):6745–6750, 2018a. ISSN 10916490. doi: 10.1073/pnas.1801846115.

Letten, A. D., Dhami, M. K., Ke, P. J., and Fukami, T. Species coexistence through simultaneous fluctuation-dependent mechanisms. *Proceedings of the National Academy of Sciences of the United States of America*, 115(26):6745–6750, 2018b. ISSN 10916490. doi: 10.1073/pnas.1801846115.

Li, G., Xie, C., Lu, S., Nichols, R. G., Tian, Y., Li, L., Patel, D., Ma, Y., Brocker, C. N., Yan, T., Krausz, K. W., Xiang, R., Gavrilova, O., Patterson, A. D., and Gonzalez, F. J. Intermittent Fasting Promotes White Adipose Browning and Decreases Obesity by Shaping the Gut Microbiota. *Cell Metabolism*, 26(4):672–685, 2017. ISSN 19327420. doi: 10.1016/j.cmet.2017.08.019. URL http://dx.doi.org/10.1016/j.cmet.2017.08.019.

Lin, Y. H., Bayrock, D. P., and Ingledew, W. M. Evaluation of Saccharomyces cerevisiae grown in a multistage chemostat environment under increasing levels of glucose. *Biotechnology Letters*, 24(6):449–453, 2002. doi: 10.1023/A:1014501125355.

Mackey, R. L. and Currie, D. J. The diversity-disturbance relationship: Is it generally strong and peaked? *Ecology*, 82(12):3479–3492, 2001. ISSN 00129658. doi: 10.1890/0012-9658(2001)082[3479:TDDRII]2.0.CO;2.

Merritt, J. and Kuehn, S. Frequency- and Amplitude-Dependent Microbial Population Dynamics during Cycles of Feast and Famine. *Physical Review Letters*, 121(9):098101, 8 2018. ISSN 0031-9007. doi: 10.1103/PhysRevLett.121.098101. URL https://link.aps.org/doi/10.1103/PhysRevLett.121.098101.

Miller, A. D., Roxburgh, S. H., and Shea, K. How frequency and intensity shape diversity-disturbance relationships. *Proceedings of the National Academy of Sciences of the United States of America*, 108(14):5643–5648, 2011. ISSN 10916490. doi: 10.1073/pnas.1018594108.

Mougi, A. and Kondoh, M. Diversity of Interaction Types and Ecological Community Stability. *Science*, 337 (6092):349–351, 2012. ISSN 0036-8075. doi: 10.1126/science.1220529. URL http://www.sciencemag.org/cgi/doi/10.1126/science.1220529.

Novick, A. and Szilard, L. Experiments with the Chemostat on Spontaneous Mutations of Bacteria. *Proceedings of the National Academy of Sciences*, 36(12):708–719, 12 1950. ISSN 0027-8424. doi: 10.1073/pnas.36.12.708. URL http://www.pnas.org/cgi/doi/10.1073/pnas.36.12.708.

Novozhilov, A. S., Karev, G. P., and Koonin, E. V. Biological applications of the theory of birth-and-death processes. *Briefings in Bioinformatics*, 7(1):70–85, 3 2006. ISSN 1467-5463. doi: 10.1093/bib/bbk006. URL https://academic.oup.com/bib/article/7/1/70/263777.

Piccardi, P., Vessman, B., and Mitri, S. Toxicity drives facilitation between 4 bacterial species. *Proceedings of the National Academy of Sciences*, 116(32):15979–15984, 2019. ISSN 0027-8424. doi: 10.1073/pnas.1906172116.

Rodríguez-Verdugo, A., Vulin, C., and Ackermann, M. The rate of environmental fluctuations shapes ecological dynamics in a two-species microbial system. *Ecology Letters*, 22(5):838–846, 5 2019. ISSN 1461-023X. doi: 10.1111/ele.13241. URL http://doi.wiley.com/10.1111/ele.13241.

Roesch, L. F., Fulthorpe, R. R., Riva, A., Casella, G., Hadwin, A. K., Kent, A. D., Daroub, S. H., Camargo, F. A., Farmerie, W. G., and Triplett, E. W. Pyrosequencing enumerates and contrasts soil microbial diversity. *ISME Journal*, 1(4):283–290, 2007. ISSN 17517362. doi: 10.1038/ismej.2007.53.

Schreiber, S., Levine, J., Godoy, O., Kraft, N., and Hart, S. Does deterministic coexistence theory matter in a finite world? *bioRxiv*, 2020. doi: 10.1101/290882.

Smits, S. A., Leach, J., Sonnenburg, E. D., Gonzalez, C. G., Lichtman, J. S., Reid, G., Knight, R., Manjurano, A., Changalucha, J., Elias, J. E., Dominguez-Bello, M. G., and Sonnenburg, J. L. Seasonal cycling in the gut microbiome of the Hadza hunter-gatherers of Tanzania. *Science*, 357(6353):802–805, 2017. ISSN 10959203. doi: 10.1126/science.aan4834.

Srinivasan, S. and Kjelleberg, S. Cycles of famine and feast: The starvation and outgrowth strategies of a marine Vibrio. *Journal of Biosciences*, 23(4):501–511, 1998. ISSN 02505991. doi: 10.1007/BF02936144.

Sun, Z., Koffel, T., Stump, S. M., Grimaud, G. M., and Klausmeier, C. A. Microbial cross-feeding promotes multiple stable states and species coexistence, but also susceptibility to cheaters. *Journal of Theoretical Biology*, 465:63–77, 2019. ISSN 00225193. doi: 10.1016/j.jtbi.2019.01.009. URL https://linkinghub.elsevier.com/retrieve/pii/S0022519319300104.

Taitelbaum, A., West, R., Assaf, M., and Mobilia, M. Population Dynamics in a Changing Environment: Random versus Periodic Switching. *Physical Review Letters*, 125(4):048105, 7 2020. ISSN 0031-9007. doi: 10.1103/PhysRevLett.125.048105. URL https://link.aps.org/doi/10.1103/PhysRevLett.125.048105.

Tecon, R., Mitri, S., Ciccarese, D., Or, D., van der Meer, J. R., and Johnson, D. R. Bridging the Holistic-Reductionist Divide in Microbial Ecology. *mSystems*, 4(1):17–21, 2019. ISSN 2379-5077. doi: 10.1128/msystems.00265-18.

Thaiss, C. A., Zeevi, D., Levy, M., Zilberman-Schapira, G., Suez, J., Tengeler, A. C., Abramson, L., Katz, M. N., Korem, T., Zmora, N., Kuperman, Y., Biton, I., Gilad, S., Harmelin, A., Shapiro, H., Halpern, Z., Segal, E., and Elinav, E. Transkingdom control of microbiota diurnal oscillations promotes metabolic homeostasis. *Cell*, 159(3):514–529, 2014. ISSN 10974172. doi: 10.1016/j.cell.2014.09.048. URL http://dx.doi.org/10.1016/j.cell.2014.09.048.

Vasi, F., Travisano, M., and Lenski, R. E. Long-term experimental evolution in Escherichia coli. II.Changes in life-history traits during adaptation to a seasonal environment. *American Naturalist*, 144(3):432–456, 1994. ISSN 00030147. doi: 10.1086/285685. URL https://www.jstor.org/stable/2462954.

West, R. and Mobilia, M. Fixation properties of rock-paper-scissors games in fluctuating populations. *Journal of Theoretical Biology*, 491:110135, 4 2020. ISSN 00225193. doi: 10.1016/j.jtbi.2019.110135. URL http://dx.doi.org/10.1016/j.jtbi.2019.110135.

West, R., Mobilia, M., and Rucklidge, A. M. Survival behavior in the cyclic Lotka-Volterra model with a randomly switching reaction rate. *Physical Review E*, 97(2):022406, 2 2018. ISSN 2470-0045. doi: 10.1103/PhysRevE.97.022406. URL https://link.aps.org/doi/10.1103/PhysRevE.97.022406.

Wienand, K., Frey, E., and Mobilia, M. Evolution of a Fluctuating Population in a Randomly Switching Environment. *Physical Review Letters*, 119(15):158301, 10 2017. ISSN 0031-9007. doi: 10.1103/PhysRevLett.119.158301. URL https://link.aps.org/doi/10.1103/PhysRevLett.119.158301.

Wienand, K., Frey, E., and Mobilia, M. Eco-evolutionary dynamics of a population with randomly switching carrying capacity. *Journal of the Royal Society Interface*, 15(145):20180343, 8 2018. ISSN 17425662. doi: 10.1098/rsif.2018.0343. URL https://royalsocietypublishing.org/doi/10.1098/rsif.2018.0343.

Xavier, J. B., Picioreanu, C., and Van Loosdrecht, M. C. M. A framework for multidimensional modelling of activity and structure of multispecies biofilms. *Environmental Microbiology*, 7(8):1085–1103, 2005. ISSN 14622912. doi: 10.1111/j.1462-2920.2005.00787.x.

Zhao, Y. and Lin, Y. H. Growth of Saccharomyces cerevisiae in a chemostat under high glucose conditions. *Biotechnology Letters*, 25(14):1151–1154, 2003. ISSN 01415492. doi: 10.1023/A:1024577414157.

Zuñiga, C., Li, C.-T., Yu, G., Al-Bassam, M. M., Li, T., Jiang, L., Zaramela, L. S., Guarnieri, M., Betenbaugh, M. J., and Zengler, K. Environmental stimuli drive a transition from cooperation to competition in synthetic phototrophic communities. *Nature Microbiology*, 4(12):2184–2191, 12 2019. ISSN 2058-5276. doi: 10.1038/s41564-019-0567-6. URL http://www.nature.com/articles/s41564-019-0567-6.

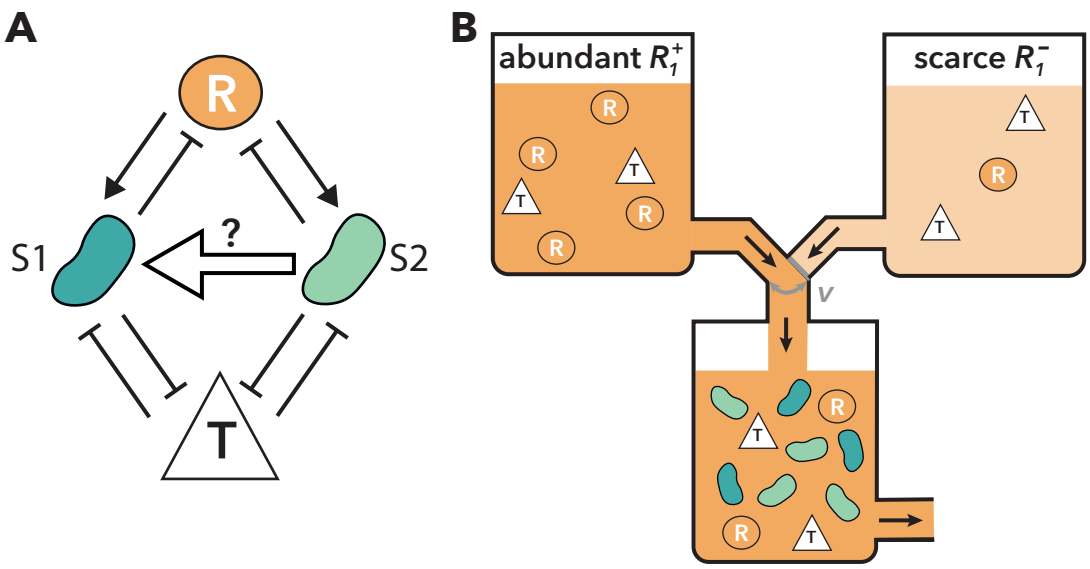

Figure 1: Schematic illustration of the model

A chemostat model with environmental switching. A: Interaction network when $N = 2$. A $\rightarrow$ B represents that A increases B while A $\dashv$ B represents that A decreases B. Two species compete for the same resource (R in a circle) but are killed by the same toxic compound (T in a triangle). As a proxy for species interactions, we follow the net effect of species 2 on species 1 (large arrow from species 2 to 1) – due to resource competition plus facilitation by detoxification – which can be environmentally mediated. B: An example of a chemostat model with environmental switching and $N = 2$. Environmental switching is realized by changing the media flowing into a chemostat. In this example, the current environmental condition is $\xi = 1$ (abundant resource supply R_1^+).

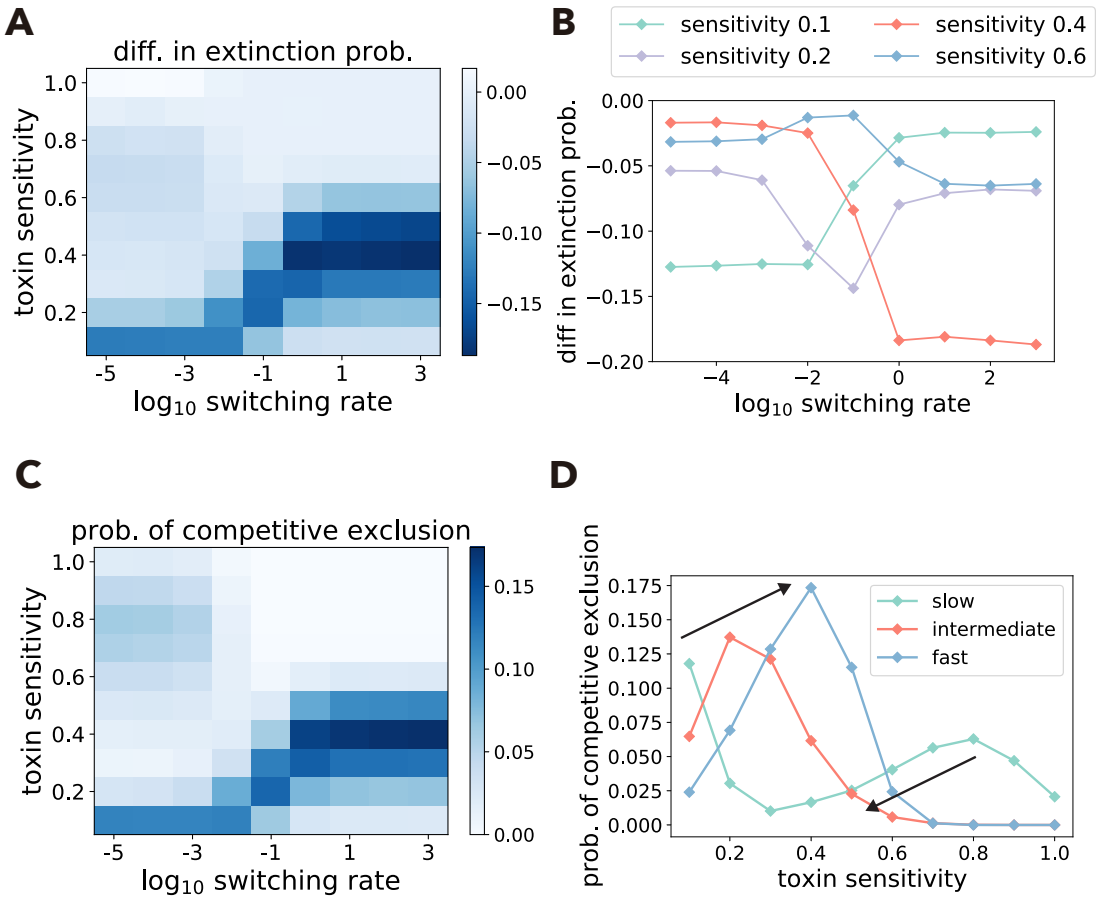

Figure 2: Species interaction strength changes differently over the switching rate

A: The effect of species 2 on species 1's extinction probability $\Delta P\left(s_1(T_{end})=0\right)$ (Eq 7) changes over the switching rate ν and the toxin sensitivity $\delta=\delta_{11}=\delta_{21}$. In most of the parameter space, species 2 has a negative effect on species 1. B: Some illustrative examples from panel A plotted differently to show how ΔP changes over the switching rate at given toxin sensitivities. The difference in extinction probability can monotonically increase ($\delta=0.1$, green), monotonically decrease ($\delta=0.4$, red), or non-monotonically change with a minimum ($\delta=0.2$, purple) or a maximum ($\delta=0.6$, blue) value at an intermediate switching rate. C: Probability that species 2 persists but species 1 goes extinct (i.e., competitive exclusion) over switching rate and toxin sensitivity. D: competitive exclusion probabilities over the toxin sensitivity, when the environmental switching rate is slow ($\nu=10^{-5}$), intermediate ($\nu=10^{-1}$), or fast ($\nu=10^{3}$).

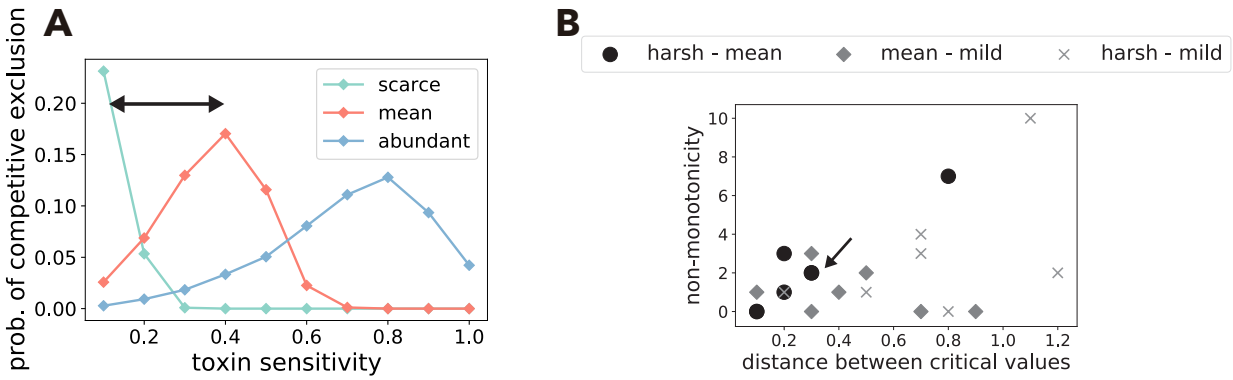

Figure 3: Competitive exclusion explains changes in species interactions

Analysis on competitive exclusion predicts at which toxin sensitivity the species interaction can change non-monotonically. A: In the absence of environmental switching, the competitive exclusion probability (i.e., probability that species 2 excludes species 1) is uni-modal over the switching rate. The toxin sensitivities giving the peak values (critical toxin sensitivities) depend on the resource supply: scarce $R_1 = R_1^-$ (green), mean $R_1 = \langle R_1 \rangle$ (red), or abundant $R_1 = R_1^+$ (blue). B: The number of times we observe non-monotonic species interactions across the explored parameter range changes with the distance between the two critical toxin sensitivities, depending on where distances are measured (between harsh and mean environments: dots, between mean and mild: environment diamonds, and between harsh and mild environments: crosses). These three distances were measured in each of the following seven scenarios: three different scenarios of environmental switching (Table 1 and Appendix 4) and four environmental switching scenario 1s with changing amounts of resource supplies (Appendix 5). The correlation is only significantly positive for the distance between scarce resource or abundant toxin supplies (i.e., harsh environments) and mean resource/toxin supplies (Spearman's $\rho = 0.77$, P-value: 0.043). The distance corresponding to the scenario analyzed in the main text is shown by the black arrow in panel A, where scarce resources are considered to be a harsh environment (dot indicated by the arrow in panel B).

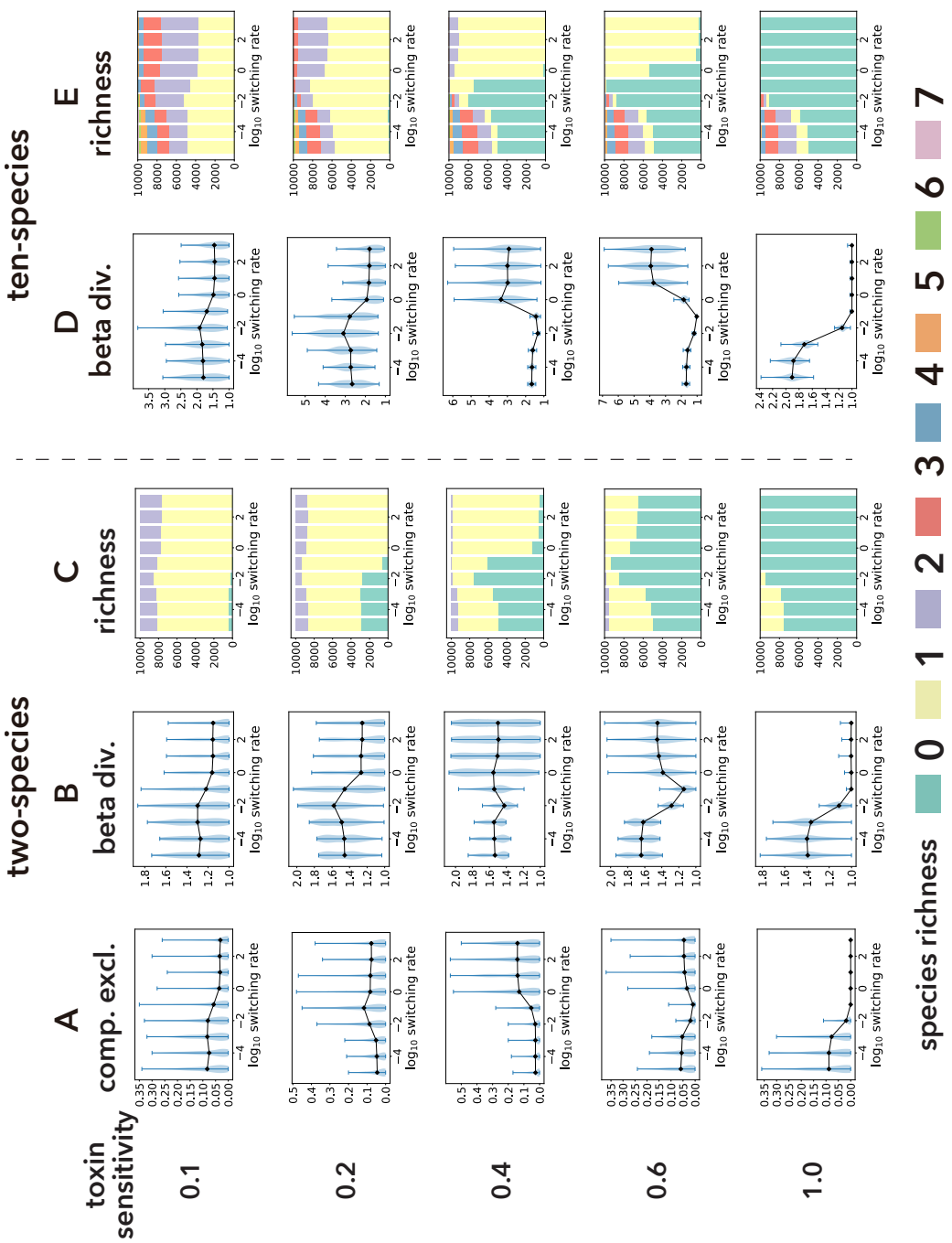

Figure 4: Comparison of competitive exclusion and beta diversity

Competitive exclusion probabilities (column A), beta diversities (column B), and species richness (column C) over the switching rate in two-species communities. Here, competitive exclusion refers the event where the slower-growing species excludes the faster-growing species. Columns D and E show the beta diversity and species richness in ten-species communities, respectively. In the plots of competitive exclusion probability and beta diversity, the black lines show the means and blue areas represent the probability distributions calculated from 10'000 simulations (100 beta diversity and each of them from 100 replicate runs). Each color in the species richness plots represents the proportion of 10'000 runs where at the end of the run there were that number of species surviving. Each row represents the mean toxin sensitivity $\bar{\delta}$ of communities in those runs.

Table 1: Different scenarios of environmental switching

Scenario	$R_i\,(\xi=1)$	$R_i\,(\xi=-1)$	$T_j\,(\xi=1)$	$T_j\,(\xi=-1)$
1	R_i^+	R_i^-	$\langle T_j \rangle$	$\langle T_j \rangle$
2	$\langle R_i \rangle$	$\langle R_i \rangle$	T_j^-	T_j^+
3	R_i^+	R_i^-	T_j^-	T_j^+